

---

# <sup>111</sup>In-Labeled CD34+ Hematopoietic Progenitor Cells in a Rat Myocardial Infarction Model

Winfried Brenner, MD<sup>1</sup>; Alexandra Aicher, MD<sup>2</sup>; Thomas Eckey<sup>1</sup>; Schirin Massoudi, MD<sup>1</sup>; Maaz Zuhayra, PhD<sup>1</sup>; Ulrike Koehl, PhD<sup>3</sup>; Christopher Heesch, MD<sup>2</sup>; Willm U. Kampen, MD<sup>1</sup>; Andreas M. Zeiher, MD<sup>2</sup>; Stefanie Dimmeler, PhD<sup>2</sup>; and Eberhard Henze, MD<sup>1</sup>

<sup>1</sup>Department of Nuclear Medicine, University Hospital Kiel, Kiel, Germany; <sup>2</sup>Department of Molecular Cardiology, Internal Medicine IV, University of Frankfurt, Frankfurt, Germany; and <sup>3</sup>Department of Pediatric Hematology and Oncology, University of Frankfurt, Frankfurt, Germany

---

Transplantation of progenitor cells (PCs) has been shown to improve neovascularization and left ventricular function after myocardial ischemia. The fate of transplanted PCs has been monitored by fluorescence labeling or by genetic modifications introducing reporter genes. However, these techniques are limited by the need to kill the experimental animal. The aim of this study was to radiolabel CD34<sup>+</sup> hematopoietic PCs (HPCs) with <sup>111</sup>In-oxine and to evaluate the feasibility of this in vivo method for monitoring myocardial homing of transplanted cells in a rat myocardial infarction model. **Methods:** Human HPCs were isolated from mobilized peripheral blood and labeled with <sup>111</sup>In-oxine. Labeled HPCs were injected into the cavity of the left ventricle in nude rats 24 h after induction of myocardial infarction (*n* = 4) or sham operation (*n* = 4). Scintigraphic images were acquired up to 96 h after HPC injection. After animals were killed, tissue samples of various organs were harvested to calculate tissue-specific activity and for immunostaining. **Results:** Labeling efficiency of HPCs was 32% ± 11%. According to trypan-blue staining, viability of radiolabeled HPCs was impaired by 30% after 48 and 96 h in comparison with unlabeled cells, whereas proliferation and differentiation of HPCs was nullified after 7 d, as assessed by colony-forming assays. After injection of HPCs, the specific activity ratio of heart to peripheral muscle tissue increased from 1.10 ± 0.32 in sham-operated rats to 2.47 ± 0.92 (*P* = 0.020) in infarcted rats. However, the overall radioactivity detected in the heart was only about 1%. A transient high lung uptake of 17% ± 6% was observed within the first hour after infusion of HPCs. At 24 h after injection, the initial lung activity had shifted toward liver, kidneys, and spleen, resulting in an increase of radioactivity in these organs from 37% ± 6% to 57% ± 5%. **Conclusion:** Radiolabeling with <sup>111</sup>In-oxine is a feasible in vivo method for monitoring transplanted HPCs in a rat myocardial infarction model. The potential to detect differences in myocardial homing between infarcted and normal hearts suggests that this method may provide a noninvasive imaging approach for clinical trials using transplanted HPCs in patients. Our findings, however, also demonstrated a negative effect of <sup>111</sup>In-oxine on cellular function, which resulted in complete impairment of HPC proliferation and

differentiation. For future trials in stem cell imaging with <sup>111</sup>In-oxine, therefore, it will be mandatory to carefully check for radiation-induced cell damage.

**Key Words:** CD34+ hematopoietic progenitor cells; <sup>111</sup>In-oxine; rat myocardial infarction model; cell trafficking; radiation-induced cell damage

**J Nucl Med 2004; 45:512-518**

---

**N**ovel approaches to cell therapy that may contribute to neovascularization and remodeling of acute ischemic tissue in myocardial infarction or chronic ischemic heart disease have been reported in both preclinical and clinical studies. Infusion of both ex vivo cultivated endothelial progenitor cells (EPCs) or CD34<sup>+</sup> hematopoietic progenitor cells (HPCs) improved neovascularization and left ventricular function after myocardial ischemia (1-4). However, little quantitative data on the biodistribution and in vivo kinetics of progenitor cells (PCs) have been reported. Tissue distribution of these cells has been monitored by fluorescence labeling of transplanted PCs or by genetic modifications introducing genes for fluorochromes or metabolic enzymes (5-7). Detection of fluorescence or enzyme-produced colorimetric reactions in different tissues and organs, however, is limited by the need to kill the animal, precluding the use of this technique in humans. In addition, immunohistochemical analysis of tissue sections does not allow quantification of the homing of the transplanted autologous cells to different organs and tissues to describe distribution within the whole body. Moreover, detection by immunohistochemical methods is limited in assessing the time course of cell trafficking, because it is not possible to investigate the same animal repeatedly. Thus, alternative noninvasive monitoring methods that are also applicable in patients are necessary to get additional insights in PC trafficking and homing.

Radiolabeling of cells has been widely used to monitor the fate and tissue distribution of blood cells. Imaging of leukocyte distribution, for example, is a routine clinical procedure to localize areas of inflammation (8-10). For this purpose, commercially available and commonly used <sup>111</sup>In-

---

Received Jun. 18, 2003; revision accepted Nov. 24, 2003.  
For correspondence or reprints contact: Winfried Brenner, MD, University of Washington Medical Center, Division of Nuclear Medicine, 1959 NE Pacific St., Box 356113, Seattle, WA 98195-6113.  
E-mail: winbren\_2000@yahoo.com

oxine has been proven a safe and easy-to-use radiolabel.  $^{111}\text{In}$  compounds have been applied successfully in various experimental settings to determine the biodistribution of transplanted hepatocytes (11), the migration patterns of dendritic cells (12,13), the homing of mesenchymal stem cells (14), and the physiologic recirculation of lymphocytes (15). In a first report on  $^{111}\text{In}$ -oxine-labeled EPCs, we showed the feasibility of this method for monitoring EPCs in rats after myocardial infarction (16).

The aims of this animal study, based on our previous findings for EPCs, were to radiolabel HPCs with  $^{111}\text{In}$ -oxine, monitor the biodistribution of transplanted HPCs in a rat myocardial infarction model, and investigate the impact of the labeling procedure on cellular function (1,3).

## MATERIALS AND METHODS

### Cell Preparation

CD34+ HPCs were obtained from cryopreserved samples after allogeneic transplantation of CD34-selected grafts in accordance with informed consent. Stem cells were mobilized from healthy donors with granulocyte colony-stimulating factor (CSF; 5  $\mu\text{g}/\text{kg}/\text{d}$ ), and peripheral blood stem cells (PBSC) were collected using a Cobe Spectra (Cobe Laboratories). Next, CD34+ cells were immunomagnetically selected from PBSC using the automated CliniMacs device (Miltenyi-Biotech) after labeling with CD34 antibodies (CD34 MicroBeads; Miltenyi-Biotech) for 30 min at room temperature as described previously (17). Enrichment of CD34+ cells resulted in a purity of >95%, as assessed by flowcytometric analysis using CD45-fluoroisothiocyanate/CD34-phycoerythrin/7-aminoactinomycin staining. After transplantation of freshly selected grafts, small pilots were cryopreserved in liquid nitrogen using X-Vivo 10 medium (Bio Whittaker) supplemented with 10% dimethyl sulfoxide for subsequent analyses and safety control. Several years after transplantation, the anonymized pilots with the CD34+ selected cells were thawed using phosphate-buffered saline (PBS) + 1 mmol/L ethylenediaminetetraacetic acid. After spinning, cells were resuspended in RPMI + 10% fetal calf serum (FCS) + 20 ng/mL stem cell factor (SCF; R&D) + 20 ng/mL interleukin-3 (IL-3; R&D) and kept at 5%  $\text{CO}_2$  and 37°C for 1 h until experimental use.

### Radiolabeling

HPCs were thawed and preactivated by stimulation with 20 ng/mL SCF and IL-3 in RPMI + 10% FCS. After 2 washes with PBS, HPCs were incubated with 30 MBq  $^{111}\text{In}$ -oxine (37 MBq/mL; Nycomed Amersham) for 60 min at 37°C in serum-free medium. To remove excess unbound radioactivity, all cells were washed twice with serum-free medium. Labeling efficiency was measured with a dose calibrator (Atomlab 100; Biodex Medical). Before injection, cells were resuspended in 0.5 mL of serum-free medium in 1.0-mL syringes with 27-gauge needles.

### Functional Assays

For evaluation of cellular effects of  $^{111}\text{In}$ -oxine labeling,  $1 \times 10^6/\text{mL}$  HPCs were labeled with 30 MBq  $^{111}\text{In}$ -oxine for 60 min and were then seeded into 15-mL polypropylene tubes. After 1, 24, 48, and 96 h ( $n = 3$  each), medium was removed and radiolabeled HPCs were stained by trypan-blue for assessing cell viability. Radiolabeled HPCs were compared with untreated cells to evaluate cell death induced by the radiolabel.

To further assess the influence of radiolabeling on HPC function, migration assays were performed using transwell plates (Costar) in a modified Boyden chamber with filter membranes (5  $\mu\text{m}$  pores) coated with fibronectin (20  $\mu\text{g}/\text{mL}$ ) in PBS for 30 min at 4°C. Before adding CD34+ cells to the upper compartment of the transwells, filter membranes were washed twice with Iscove medium supplemented with 10% FCS (complete medium; Biochrome). Then,  $1 \times 10^5$  CD34+ cells were added to the upper compartment in 0.1 mL of medium, and cells were allowed to migrate through the membrane toward the lower chamber in response to 0.6 mL of medium with 100 ng/mL stromal cell-derived factor (SDF-1; R&D). The transwell plates were incubated at 37°C and 5%  $\text{CO}_2$  for 2 h. Then, the filter membranes were carefully discarded, and the cells that had migrated into the lower compartment were fixed by adding 0.6 mL of 4% formaldehyde. Cells were allowed to attach to the lower plastic surface of the plates and were scored by microscopic analysis of 5 random fields.

In addition, we performed experiments on the capacity of HPCs to produce colonies on semisolid media. HPCs can proliferate into clones of differentiated progeny. CD34+ cells ( $1 \times 10^4$ ) were inoculated into 1.5 mL of semisolid methylcellulose (MethoCult; Stem-Cell Technologies) containing FCS, human SCF, human granulocyte-macrophage CSF, human IL-3, and human erythropoietin and were allowed to proliferate and differentiate into colony-forming units (CFUs). CFUs were scored after 7 d of incubation.

### Animals and Study Design

Human cells were transplanted into a xenogeneic rat model using immunodeficient athymic rnu:rnu rats (5- to 7-wk-old females,  $120 \pm 30$  g body weight; Charles River). Animals were anesthetized with intramuscular ketamine (100 mg/kg; Curamed) and midazolam (2 mg/kg; Hoffmann-LaRoche). To prevent arrhythmias after cardiac surgery, intramuscular amiodarone (5 mg/kg; Sanofi-Synthelabo) was given prophylactically. Furthermore, to reduce intra- and postoperative pain, piritramide (2 mg/kg; Janssen-Cilag) was administered. A 17-gauge endotracheal tube was inserted for volume-controlled ventilation of the animals. Open-chest cardiac surgery was performed after left thoracotomy to occlude the left anterior descending coronary artery (LAD) by passing a 5-0 suture around the LAD just under the tip of the left auricle ( $n = 4$ ). Sham-treated animals underwent left thoracotomy and incision of the pericardium only ( $n = 4$ ). After the chest wound was closed, rats were allowed to recover for 24 h before injection of HPCs.

$^{111}\text{In}$ -Oxine-labeled HPCs with a mean activity of  $9.3 \pm 3.4$  MBq were administered using an x-ray-assisted transdiaphragmatic approach for intracavitary administration into the left ventricle of either sham-treated ( $n = 4$ ) or infarcted ( $n = 4$ ) rats. Because intracoronary application cannot be performed in rats, intracavitary administration of HPCs was considered the closest approach possible to the intracoronary cell administration in patient studies. During this procedure, contrast medium (Isovist; Schering) was injected to confirm proper left ventricular position of the needle using x-ray control.

Three additional animals received pure  $^{111}\text{In}$ -oxine as controls to assess the distribution of free  $^{111}\text{In}$ -oxine. In another 3 animals with no surgical pretreatment, radiolabeled HPCs were administered to exclude the surgical procedure as a reason for cardiac homing.

For scintigraphic imaging, animals were anesthetized with ketamine and midazolam. Planar whole-body pinhole images and spot images of the thorax were acquired over 30 min at 1, 24, 48, and 96 h after cell administration using a double-head  $\gamma$ -camera (ECAM; Siemens) equipped with a pinhole collimator with an insert for medium energy. The energy windows were centered at  $171 \text{ keV} \pm 10\%$  and  $245 \text{ keV} \pm 10\%$ , and images were stored in a  $512 \times 512$  matrix.

After the last image acquisition, animals were killed. All animal experiments were performed with approved consent by the local Animal Research Committee in accordance with both federal animal protection and radiation protection laws (V 252-72241.122-17).

### Tissue Preparation and Immunostaining

To detect CD34+ cells in histologic sections, we used the green cell tracker 5-chloromethylfluoresceindiacetate (CMFDA; Molecular Probes) for colabeling. After the rats were killed, transverse slices of the base, midregion, and apex of the hearts as well as tissue samples from other organs, such as skeletal muscles, lungs, kidneys, liver, bones, and spleen, were obtained. All specimens were weighed, and the counting rate was measured in a lead-shielded and calibrated well counter (LB 5310; Berthold) to calculate the specific activity per gram of tissue sample per megabecquerel of injected activity after correction for radioactive decay. Organ samples were mounted in TissueTek OCT compound freezing medium (Sakura) and snap frozen in 2-methylbutane prechilled by liquid nitrogen. Sections of  $5 \mu\text{m}$  were cut and examined for human cells. Destruction of cardiomyocytes as a result of myocardial infarction was visualized by staining of myocytes with  $\alpha$ -sarcomeric actinin (Sigma), followed by goat-anti-mouse Cy3 (red; Dianova). Nuclei were stained with TO-PRO-3 (blue; Molecular Probes), and sections were analyzed using a confocal microscope (LSM 510; Zeiss).

### Statistical Analysis

Data presented in the results represent mean  $\pm$  SD. The Student *t* test for unpaired data was used to evaluate statistical differences between rat subgroups, with  $P < 0.05$  considered to be statistically significant.

## RESULTS

### HPC Labeling with $^{111}\text{In}$ -Oxine

To test the efficiency of the labeling procedure, HPCs were incubated with 30 MBq  $^{111}\text{In}$ -oxine in serum-free

medium for 60 min. Incorporation of  $^{111}\text{In}$ -oxine in percentage of added activity yielded a mean labeling efficiency of  $31.9\% \pm 11.0\%$  after 60 min.

Next, we investigated whether the labeling affects cell viability. We counted the number of dead cells by trypan-blue staining in both radiolabeled and unlabeled cells at 1, 24, 48, and 96 h (Fig. 1). Up to 24 h after radiolabeling, no significant differences were observed, whereas at 48 ( $P = 0.030$ ) and 96 h ( $P = 0.011$ ), an increased number of dead cells was found after radiolabeling of HPCs ( $n = 3$  each).

To check specific cellular functions, we performed migration studies with HPCs in a modified Boyden chamber in response to the chemotactic SDF-1. A significant reduction of SDF-1-induced migration was already detected 24 h after radiolabeling, resulting in a decrease in the number of migrated radiolabeled HPCs to 74.2% of the number of unlabeled control cells ( $P < 0.001$ ;  $n = 3$  each). At 48 h, SDF-1-induced migration was nullified in radiolabeled cells and reduced to 59.8% of the initial value in unlabeled cells.

In addition, we performed experiments on the capacity of  $^{111}\text{In}$ -oxine-labeled HPCs to produce colonies on semisolid media. HPCs were labeled for 1 h and then allowed to proliferate and differentiate into CFUs, which were scored after 7 d. Although untreated cells showed  $164 \pm 55$  CFUs per 10,000 inoculated HPCs, no CFUs were detected in radiolabeled cells ( $n = 3$  each).

Finally, we checked the activity of  $^{111}\text{In}$  in the supernatants as well as in the cells to determine the loss of  $^{111}\text{In}$  from the cells into the supernatant. We found that  $33.5\% \pm 10.3\%$ ,  $63.9\% \pm 0.9\%$ , and  $74.5\% \pm 10.2\%$  of  $^{111}\text{In}$  initially incorporated into HPCs was released into the supernatant after 24, 48, and 96 h, respectively.

### Distribution of Radiolabeled HPCs

After  $^{111}\text{In}$ -oxine-labeled human HPCs were administered directly into the left ventricular cavity of infarcted or sham-operated rats, a high tracer accumulation of  $37\% \pm 6\%$  of the injected activity was found in the liver, kidneys, and spleen at 1 h after injection (Fig. 2). A transient high lung uptake of  $17\% \pm 6\%$  was observed within the first hour after infusion of HPCs (Fig. 2). At 24 h after injection,

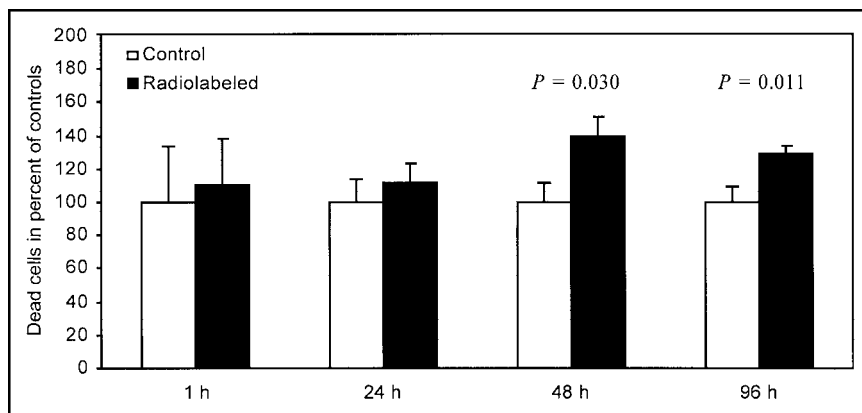


**FIGURE 1.** Trypan-blue staining. Values are given as percentages of dead cells of controls as determined by counting 5 microscopic random fields of view ( $n = 3$  each). Significant differences were found at 48 and 96 h after radiolabeling.

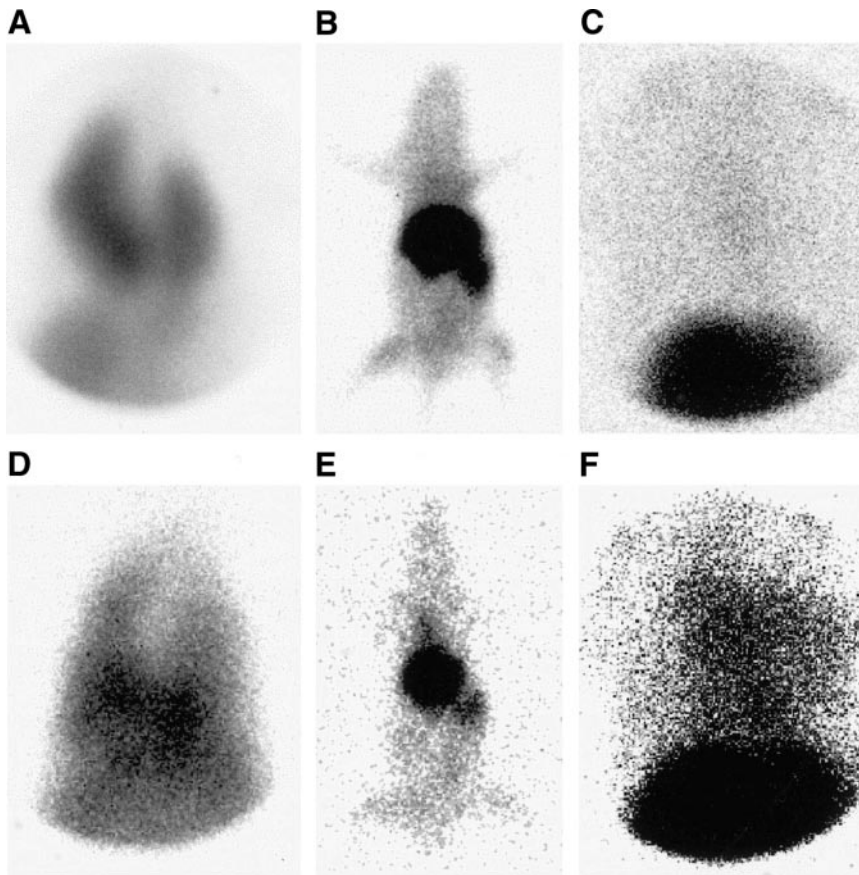


**FIGURE 2.** Pinhole images of nude rats without (A–C) or with (D–F) myocardial infarction after injection of  $^{111}\text{In}$ -oxine-labeled HPCs into the left ventricular cavity. At 1 h after injection, a high lung uptake was visible on the spot images of the chest and abdomen (A and D), but was no longer detectable on images at 24 (B and E) and 96 (C and F) h after injection. The spot images of the chest and abdomen after 96 h clearly showed significant differences in cardiac uptake between infarcted (F) and sham-operated (C) animals.

the initial lung activity was no longer detectable. It had been shifted to liver, kidneys, and spleen, resulting in an increase of radioactivity in these organs to  $57\% \pm 5\%$  during the first 24 h. Tracer distribution then remained stable up to 96 h after injection. At all time points in rats with myocardial infarction, a diffuse heart uptake could be detected, whereas no activity accumulation was found within the heart in sham-operated controls (Fig. 2). The pinhole collimator provided a sufficiently high resolution to discriminate the heart from liver and spleen, depicting ischemia-induced heart uptake in infarcted rats.

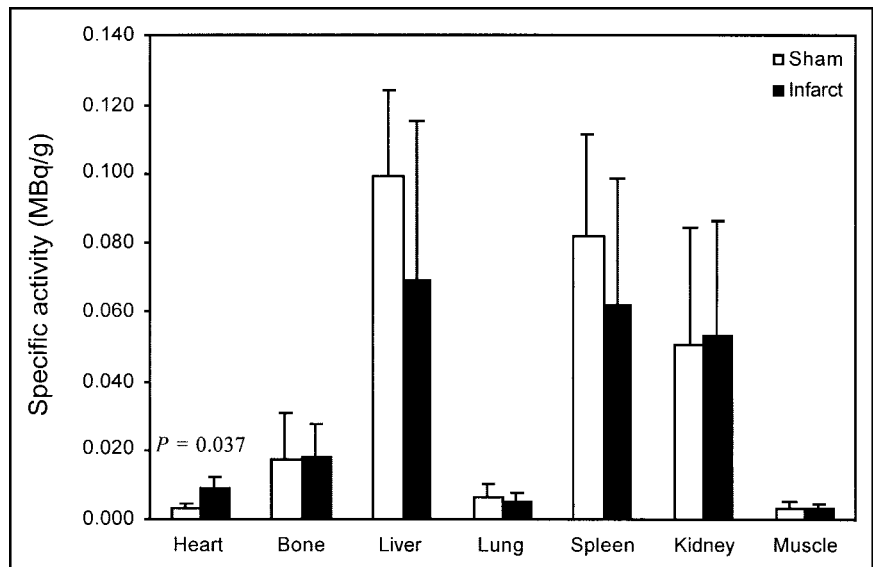
After 96 h, animals were killed, and the specific radioactivity per gram of tissue per megabecquerel of injected activity was measured in different tissues. Consistent with the in vivo images, liver, spleen, and kidneys revealed the highest specific tissue activities (Fig. 3). Because the specific activity of skeletal muscle was a constant parameter, we calculated the heart-to-muscle specific activity ratio (i.e., the ratio of specific radioactivity of the heart compared with peripheral skeletal muscle tissue) as a reference parameter for comparison. In sham-operated animals, the heart-to-muscle specific activity ratio was  $1.10 \pm 0.32$ . It significantly increased to  $2.47 \pm 0.92$  ( $P = 0.020$ ) when HPCs were infused in rats with previous infarction. After correction for radioactive decay, the amount of radioactivity in the whole heart was 1% of the injected activity in infarcted rats, which correlated to  $1 \times 10^4$  HPCs.

In 3 animals treated with  $^{111}\text{In}$ -oxine alone, a high blood-pool activity was observed up to 96 h after injection as a result of the strong affinity of oxine to serum transferrin. According to the scintigrams, blood samples at 96 h showed a more than 25-fold higher specific blood activity compared with animals treated with  $^{111}\text{In}$ -oxine-labeled HPCs. In 3 rats with no surgical pretreatment, no significant differences were found for specific heart activity when compared with sham-operated animals. These findings exclude the thoracotomy itself as a reason for myocardial homing of HPCs.

#### Fluorescence Microscopy and Immunostaining

To confirm results obtained by measuring the tissue specific radioactivity, tissue sections were analyzed by immunostaining and fluorescence microscopy (Fig. 4). The human HPCs could be identified within the rat tissue by labeling with the green cell tracker CMFDA. Although HPCs were rarely found in a scattered distribution pattern in the heart of sham-operated animals, the hearts of infarcted rats revealed human cells predominantly located in the border zone of the infarction, as evidenced by visualizing neighboring cardiac myocytes with  $\alpha$ -sarcomeric actinin. In addition, tissue sections of other organs in which most of the radioactivity was detected were analyzed. HPCs were predominantly found in spleen and liver, whereas few HPCs were seen in the kidneys. In sections of thigh muscles, the

**FIGURE 3.** Distribution pattern of specific activity (megabecquerel per gram of tissue per megabecquerel of injected activity) in different tissues after left intravenous administration of  $^{111}\text{In}$ -oxine-labeled HPCs in infarcted or sham-operated nude rats. Data are given as mean  $\pm$  SD ( $n = 4$  each). Significant differences between organs of sham-operated and infarcted animals were observed only in the heart.



same scattered distribution pattern of HPCs was found as in myocardial sections of sham-operated rats.

### DISCUSSION

$^{111}\text{In}$ -Oxine is a well-known, safe, and commercially available tracer for radiolabeling and monitoring of blood cells. Inflammation scintigraphy with  $^{111}\text{In}$ -oxine-labeled leukocytes, for example, is a standard nuclear medicine procedure (8). In an earlier study on  $^{111}\text{In}$ -oxine-labeled EPCs, we demonstrated the feasibility of this *in vivo* method for monitoring EPCs in rats, finding an increased

homing of these cells in the heart after myocardial infarction (16). The results of the present study show that radiolabeling of transplanted human CD34+ HPCs (a precursor of EPCs) with  $^{111}\text{In}$ -oxine is also feasible for monitoring myocardial homing and biodistribution of these cells in rats over a somewhat limited period of 24–48 h. General limitations in dealing with  $^{111}\text{In}$ -oxine in experimental settings must be addressed. Inherent to this radiopharmaceutical are the high energy of  $^{111}\text{In}$  (171 and 245 keV), requiring medium-energy collimators with a restricted spatial resolution; limited cellular retention of  $^{111}\text{In}$ ; and irradiation of radiolabeled cells, which can result in impaired cellular viability and function.

The physical 2.8-d half-life of  $^{111}\text{In}$  allows us to monitor cell distribution for about 1 wk, which we considered a clear advantage over  $^{99\text{m}}\text{Tc}$ -labeled radiopharmaceuticals such as  $^{99\text{m}}\text{Tc}$ -hexamethylpropyleneamine (with a 6-h half-life). The limitation of  $^{111}\text{In}$ , however, is the need for medium-energy collimators. Although the spatial resolution of these collimators is rather poor, it is sufficient for clinical application in patients. However, in nude rats with a mean weight of 120 g and a heart size (about 10 mm) just in the range of or below collimator resolution, the relatively low uptake of HPCs in the heart (only 1% of injected activity) could not be distinguished from high tracer accumulation in the adjacent liver and spleen. An alternative to increasing resolution is the use of a pinhole collimator. We showed that pinhole collimators are appropriate tools to obtain a sufficiently high resolution to reliably discriminate differences between heart activities in rats with and without myocardial infarction. For an optimal resolution, however, only 1 animal can be scanned at a time, and long acquisition times of 30 min are required. For studying small animals, such as mice or rats, PET with a high spatial resolution would be the ideal imaging modality. However, when we tested the widely available  $^{18}\text{F}$ -FDG as a radiolabel, an insufficient labeling

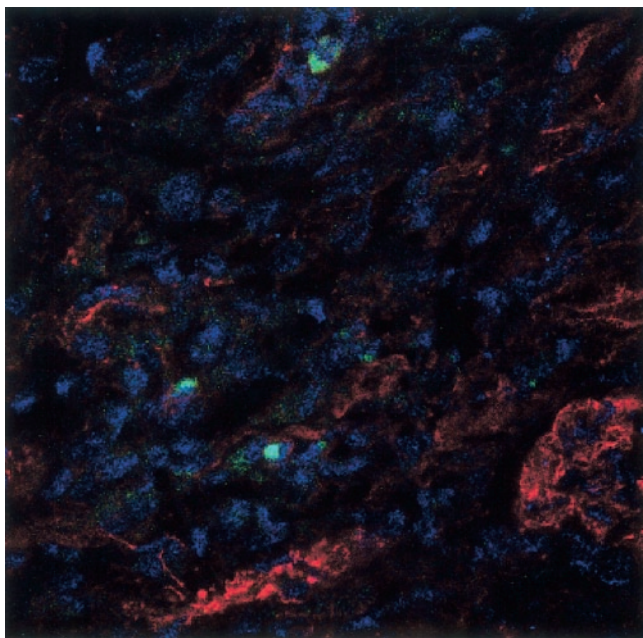


**FIGURE 4.** CMFDA cell-tracker-labeled human CD34+ HPCs (green) were identified in the infarct border zone delineated by damaged  $\alpha$ -sarcomeric actinin-positive cardiac myocytes (red). Nuclei were stained with TO-PRO-3 (blue).

efficiency of less than 10% was obtained for both EPCs and HPCs, with a high efflux rate within the first hour. In addition, the short physical half-life of 110 min for  $^{18}\text{F}$ -FDG does not seem adequate for monitoring cell trafficking.  $^{64}\text{Cu}$ -Pyruvaldehyde bis(N4-methylthiosemicarbazone) has been shown to be an alternative PET tracer for cell labeling with a potentially suitable half-life of 12.7 h (18), but this tracer is not routinely available and therefore limited to a few PET centers. Thus, to extend PC imaging from the experimental setting to clinical application, we decided to use  $^{111}\text{In}$ -labeled PCs for our studies despite the limited resolution in rats and to combine scintigraphic imaging with in vitro measurement of tissue-specific activities in the heart and other organs.

Up to 96 h after injection of radiolabeled HPCs, radioactivity was predominantly located in spleen, liver, and kidneys. Immunostaining revealed many intact HPCs in the spleen and liver. These organs have been identified as the major site for homing of immunocompetent cells (19–21). In contrast, although specific tissue activity was high in the kidneys, HPCs were rarely detectable in these organs. Loss of  $^{111}\text{In}$  from labeled cells is a well-known phenomenon and has been described as a reason for high uptake of radioactivity in liver and kidneys (22). Because the binding of this compound to intracellular structures is reversible,  $^{111}\text{In}$  is released from the labeled cells over time. For lymphocytes, a 70% loss is reported within 24 h after cell labeling (22). Lower release rates were observed in our study, with a loss of 34% of the initially cell-bound activity within 24 h into the supernatant of cultured HPCs. We consider this well-known efflux of  $^{111}\text{In}$  as the main reason for the high radioactivity uptake in the kidneys. According to this assumption, radioactivity in the kidneys was not correlated to the number of HPCs as demonstrated by immunostaining. This nonspecific tracer signal caused by the in vivo efflux of  $^{111}\text{In}$ , however, does not seem to be a major concern outside liver and kidneys, because the number of HPCs were correlated with the tissue-specific activity in the heart, muscles, lungs, and spleen. The significant difference in specific heart radioactivity between sham-operated and infarcted rats did represent the different myocardial accumulation of engrafted HPCs as shown by immunostaining.

Administration of HPCs after myocardial infarction increased the specific activity in the heart significantly. It was 2.3-fold higher in rats with infarction than in sham-operated rats. This is in accordance with previous studies, which demonstrated that tissue ischemia is a major stimulus for incorporation of circulating PCs (6,23,24). Even after infarction, however, the activity detected in the heart was quite low. Our data revealed that the absolute level of HPCs homing to the heart after myocardial infarction was about 1% of the injected activity, which corresponded to  $1 \times 10^4$  HPCs. Thus, a significantly lower myocardial uptake of HPCs was observed than the 3% for EPCs (16). Measuring the tissue-specific activity, however, results in a relative underestimation of myocardial cell incorporation at 96 h

because of the leakage of  $^{111}\text{In}$  from labeled cells. Thus, the number of incorporated cells as determined by tissue-specific activity represents the lower limit of true cell accumulation in the heart. Based on the in vitro leakage rate of 75% within 96 h, the true number of accumulated cells could be in the range of 4%.

HPCs showed a transient high lung uptake of  $17\% \pm 6\%$  immediately after intracardial infusion, a phenomenon not observed after administration of EPCs (16). As a result of this considerable lung uptake, HPC uptake in liver, spleen, and kidneys at 1 h after injection was about 50% lower than the uptake of EPCs (37% and 72%, respectively). Up to 24 h after injection, activity shifted from the lungs toward liver, spleen, and kidneys, reaching activity levels in these organs comparable to those of EPCs.

The main obstacles in dealing with  $^{111}\text{In}$ -oxine, however, are potential radiation-induced alterations of specific cellular features that have been reported for various cell types. These alterations may be caused by either irradiation or toxic effects of oxine. In activated T-lymphocytes, for example, a significant loss of cytotoxic activity and proliferation has been described with no alteration of cell viability or phenotype (25). In  $^{111}\text{In}$ -oxine-labeled activated neutrophils, upregulated adhesion and phagocytosis rates in addition to a decreased chemotaxis were found in comparison with unlabeled cells (26). Therefore, in our previous study it was an important finding that in EPCs  $^{111}\text{In}$ -oxine did not significantly affect cell viability, proliferation, migration capacity, or receptor-mediated 1,1'-dioctadecyl-3,3',3'-tetramethylindocarbocyanine-labeled acetylated low-density lipoprotein (DiLDL) uptake (16). These findings suggested that  $^{111}\text{In}$ -oxine-labeled human EPCs maintain their characteristic features. Different results, however, were obtained in HPCs, which are less differentiated than EPCs. Although the in vitro viability of radiolabeled HPCs, as measured by trypan-blue staining, was impaired by only about 30% in comparison with unlabeled cells after 48 and 96 h, proliferation and differentiation, as assessed by colony-forming assays, were nullified after 7 d of incubation. The migratory capacity in radiolabeled HPCs was reduced after 24 h and completely suppressed after 48 h. Thus, EPCs seem to be much more resistant to radiation-induced damage than are immature multipotent HPCs. Also contributing to the increased radiosensitivity of HPCs may be the fact that in this study we used HPCs that were frozen until clinical use. Nevertheless, HPCs were incorporated into the infarcted myocardium as shown by measurement of the heart-specific activity and by immunostaining. Moreover, HPC trafficking with a significant shift of activity from the lungs to liver and spleen within the first 24 h after injection could be demonstrated. Thus,  $^{111}\text{In}$ -oxine-labeled human HPCs can be used to monitor cell trafficking at least up to 24 h after injection. For cell therapy studies, however, radiolabeled HPCs do not seem suitable because of complete impairment of cell proliferation and differentiation. Only a small portion of HPCs may be radiolabeled with

<sup>111</sup>In-oxine if this imaging approach is planned for clinical studies on HPC therapy to document the myocardial homing of transplanted cells. In summary, our results clearly demonstrated the impact of <sup>111</sup>In-oxine on cell proliferation and cellular function, which can vary substantially between different PC types. In future patient trials on stem cell imaging it will be mandatory to carefully screen for radiation-induced damage and impairment of cellular function.

## CONCLUSION

The results of this animal study demonstrated that <sup>111</sup>In-oxine is a usable tracer for in vivo monitoring of transplanted CD34+ HPCs in a rat model of myocardial infarction. The potential of this method to detect differences in myocardial homing between infarcted and normal rat hearts, as proven by immunohistochemical staining, suggests that radiolabeling of transplanted HPCs with <sup>111</sup>In-oxine may provide a noninvasive imaging approach in patients. This study, however, also demonstrated the negative impact of <sup>111</sup>In-oxine, resulting in complete impairment of HPC proliferation and differentiation, which is in contrast to our previous experience with <sup>111</sup>In-oxine in more differentiated EPCs. Thus, the results of this study made clear that for future trials on stem cell imaging it will be mandatory to carefully check for radiation-induced cell damage.

## ACKNOWLEDGMENTS

We thank Christiane Mildner-Rihm and Marion Muhly-Reinholz (Molecular Cardiology, University of Frankfurt, Germany), and Kerstin Brötzmann (Department of General and Thoracic Surgery, University of Kiel, Germany), for excellent technical assistance. We also thank Dr. Hans-Ulrich Wottge and his team from the Animal Center at the University Hospital Kiel for providing excellent animal care service. We thank Rosemarie Grams (Department of Obstetrics and Gynecology, University of Kiel) for her support. We are grateful for the use of the animal laboratory facilities of the Department of General and Thoracic Surgery and the laboratory facilities of the Department of Obstetrics and Gynecology, both at the University Hospital Kiel, and the radioisotope laboratory of the Department of Nuclear Medicine at the University of Frankfurt. This work was supported by a research grant from the University of Kiel, by a young investigator grant from the University of Frankfurt, and by a research grant (Di 600/4-1) from the Deutsche Forschungsgemeinschaft.

## REFERENCES

1. Kawamoto A, Gwon HC, Iwaguro H, et al. Therapeutic potential of ex vivo expanded endothelial progenitor cells for myocardial ischemia. *Circulation*. 2001;103:634–637.
2. Assmus B, Schachinger V, Teupe C, et al. Transplantation of progenitor cells and regeneration enhancement in acute myocardial infarction (TOPCARE-AMI). *Circulation*. 2002;106:3009–3017.

3. Kocher AA, Schuster MD, Szabolcs MJ, et al. Neovascularization of ischemic myocardium by human bone-marrow-derived angioblasts prevents cardiomyocyte apoptosis, reduces remodeling and improves cardiac function. *Nat Med*. 2001;7:430–436.
4. Stamm C, Westphal B, Kleine HD, et al. Autologous bone-marrow stem-cell transplantation for myocardial regeneration. *Lancet*. 2003;361:11–12.
5. Kalka C, Masuda H, Takahashi T, et al. Transplantation of ex vivo expanded endothelial progenitor cells for therapeutic neovascularization. *Proc Natl Acad Sci USA*. 2000;97:3422–3427.
6. Shintani S, Murohara T, Ikeda H, et al. Augmentation of postnatal neovascularization with autologous bone marrow transplantation. *Circulation*. 2001;103:897–903.
7. Zhang ZG, Zhang L, Jiang Q, Chopp M. Bone marrow-derived endothelial progenitor cells participate in cerebral neovascularization after focal cerebral ischemia in the adult mouse. *Circ Res*. 2002;90:284–288.
8. Becker W, Meller J. The role of nuclear medicine in infection and inflammation. *Lancet Infect Dis*. 2001;1:326–333.
9. Rennen HJ, Boerman OC, Oyen WJ, Corstens FH. Imaging infection/inflammation in the new millennium. *Eur J Nucl Med*. 2001;28:241–252.
10. Seabold JE, Forstrom LA, Schauwecker DS, et al. Procedure guideline for indium-111-leukocyte scintigraphy for suspected infection/inflammation. Society of Nuclear Medicine. *J Nucl Med*. 1997;38:997–1001.
11. Bohnen NI, Charron M, Reyes J, et al. Use of indium-111-labeled hepatocytes to determine the biodistribution of transplanted hepatocytes through portal vein infusion. *Clin Nucl Med*. 2000;25:447–450.
12. Eggert AA, Schreurs MW, Boerman OC, et al. Biodistribution and vaccine efficiency of murine dendritic cells are dependent on the route of administration. *Cancer Res*. 1999;59:3340–3345.
13. Mackensen A, Krause T, Blum U, et al. Homing of intravenously and intralymphatically injected human dendritic cells generated in vitro from CD34+ hematopoietic progenitor cells. *Cancer Immunol Immunother*. 1999;48:118–122.
14. Gao J, Dennis JE, Muzic RF, Lundberg M, Caplan AI. The dynamic in vivo distribution of bone marrow-derived mesenchymal stem cells after infusion. *Cells Tissues Organs*. 2001;169:12–20.
15. Wagstaff J, Gibson C, Thatcher N, et al. Human lymphocyte traffic assessed by indium-111 oxine labelling: clinical observations. *Clin Exp Immunol*. 1981;43:443–449.
16. Aicher A, Brenner W, Zuhayra M, et al. Assessment of the tissue distribution of transplanted human endothelial progenitor cells by radioactive labeling. *Circulation*. 2003;107:2134–2139.
17. Koehl U, Zimmermann S, Esser R, et al. Autologous transplantation of CD133 selected haematopoietic progenitor cells in a paediatric patient with relapsed leukemia. *Bone Marrow Transplantation*. 2002;29:927–930.
18. Adonai N, Nguyen KN, Walsh J, et al. Ex vivo cell labeling with <sup>64</sup>Cu-pyruvaldehyde-bis(N4-methylthiosemicarbazone) for imaging cell trafficking in mice with positron-emission tomography. *Proc Natl Acad Sci USA*. 2002;99:3030–3035.
19. Hendriks PJ, Martens CM, Hagenbeek A, Keij JF, Visser JW. Homing of fluorescently labeled murine hematopoietic stem cells. *Exp Hematol*. 1996;24:129–140.
20. Iezzi G, Scheidegger D, Lanzavecchia A. Migration and function of antigen-primed non-polarized T lymphocytes in vivo. *J Exp Med*. 2001;193:987–993.
21. Patel SS, Thiagarajan R, Willerson JT, Yeh ET. Inhibition of alpha4 integrin and ICAM-1 markedly attenuate macrophage homing to atherosclerotic plaques in ApoE-deficient mice. *Circulation*. 1998;97:75–81.
22. Kuyama J, McCormack A, George AJ, et al. Indium-111 labelled lymphocytes: isotope distribution and cell division. *Eur J Nucl Med*. 1997;24:488–496.
23. Shintani S, Murohara T, Ikeda H, et al. Mobilization of endothelial progenitor cells in patients with acute myocardial infarction. *Circulation*. 2001;103:2776–2779.
24. Takahashi T, Kalka C, Masuda H, et al. Ischemia- and cytokine-induced mobilization of bone marrow-derived endothelial progenitor cells for neovascularization. *Nat Med*. 1999;5:434–438.
25. Botti C, Negri DR, Seregni E, et al. Comparison of three different methods for radiolabelling human activated T lymphocytes. *Eur J Nucl Med*. 1997;24:497–504.
26. Bertrand-Caix J, Freyburger G, Bordenave L, et al. Functional upregulation of granulocytes labeled with technetium-99m-HMPAO and indium-111-oxinate. *J Nucl Med*. 1996;37:863–868.